In situ monitoring of block copolymer self-assembly through controlled dialysis with light and neutron scattering detection

Martin Fauquignon, Lionel Porcar, Annie Brûlet, Jean-François Le Meins, Olivier Sandre, Jean-Paul Chapel, Marc Schmutz, Christophe Schatz

In situ monitoring of block copolymer self-assembly through controlled dialysis with light and neutron scattering detection

Martin Fauquignon,* Lionel Porcar, Annie Brûlet, Jean-François Le Meins, Olivier Sandre, Jean-Paul Chapel, Marc Schmutz, and Christophe Schatz*

ABSTRACT: Solution self-assembly of amphiphilic block copolymers (BCs) is typically performed by solvent to water exchange. However, BC assemblies are often trapped in metastable states depending on the mixing conditions, such as the magnitude and rate of water addition. BC self-assembly can be performed under near thermodynamic control by dialysis which accounts for a slow and gradual water addition. In this communication we report the use of a dialysis cell specifically designed to continuously monitor by dynamic light scattering and small-angle neutron scattering the morphological changes of PDMS-*b*-PEG BCs during THF to water exchange. The complete phase diagrams of equilibrium structures can then be established. Spherical micelles first form before evolving to rod-like micelles and vesicles, decreasing the total interfacial area of aggregates in response to increasing interfacial energy. The dialysis kinetics can be adapted to the time scale of self-assembly by modifying the membrane pore size. The approach described herein should be relevant in polymer self-assembly and in supramolecular chemistry in general to better understand the interplay between thermodynamics and kinetics in aggregate formation.

Amphiphilic block copolymers in solution can generate a variety of self-assembled structures depending on block length and chemical composition.[1–4] Compared to surfactants which self-assemble into equilibrium micellar structures, BC assemblies are often trapped in long-lived metastable states due to slow polymer chain dynamics associated with large molecular weight, hydrophobicity or glassiness of polymers.[5–12] As a consequence, relaxation mechanisms such as chain insertion/expulsion and micelle fusion/fission are considerably weakened for BC systems.[6,13] BC self-assembly can be facilitated by dissolving the block copolymer in a good solvent for both blocks before adding a selective solvent, mainly water, that is good for one block and poor for the other. The resulting aggregate morphologies are related to the water content and polymer concentration, which can be depicted by phase diagrams obtained through turbidity, microscopy observations[14,15] and more recently by computer simulation.[16,17] A recurring issue with the solvent exchange method is the equilibrium state of BC aggregates, which depends not only on the final water content but also on the magnitude and rate of the water jump.[14,18–20] In order to promote the formation of equilibrium morphologies, as expected for phase diagrams, water should be added slowly and gradually, by analogy with the conditions used for annealing in bulk studies.[21] A fast and large water jump can lead to kinetically arrested morphologies, which is the basis to form BC nanoparticles by the so-called flash nanoprecipitation technique.[22,23] Mixing homogeneity is another important parameter to obtain BC aggregates with uniform morphology and size, as shown from antisolvent crystallization studies.[24] In order to achieve slow and homogeneous mixing conditions, the mixing process should preferably rely on solvent interdiffusion rather than convection.[25] Microfluidic technology based on the principle of flow focusing[26] allows for such mixing conditions, but is inherently limited to short time scales of self-assembly (< 10 s), which is insufficient for some BC systems to reach their equilibrium morphology.[25] For example, the equilibration of BC vesicles may require several minutes depending on the composition of the solvent mixture.[14,18,25] Compared to microfluidic techniques, dialysis, which also relies on the principle of solvent interdiffusion, remains the simplest approach to achieve near-equilibrium BC self-assembly without time-scale restrictions.[27–29] However, the evolution of BC structures during dialysis cannot be monitored in real time under standard conditions using dialysis bags or tubings unless samples are collected for further analysis. Yet, this approach suffers from a few limitations: i) morphology changes occurring over narrow ranges of solvent composition can be overlooked, ii) aging of collected samples prior to analysis is inevitable, iii) sampling disrupts dialysis equilibrium.

In this study, we propose for the first time to perform kinetic monitoring of BC self-assembly during solvent exchange using a dedicated dialysis cell designed for in situ time-resolved light and neutron scattering (Figure 1A). The main objective of the communication is to highlight the capabilities of the approach, which is complementary to fast mixing methods like stopped-flow with a SAXS/SANS detection[30] previously used to study nonequilibrium morphological transition kinetics in BC self-assembly[31,32] or equilibrium chain exchange kinetics.[6,33] Polydimethylsiloxane-*block*-polyethylene glycol (PDMS-*b*-PEG) copolymer forming vesicles upon THF exchange with water was used as model BC systems. The self-assembly properties of PDMS-*b*-PEG BCs alone or with lipids has been reported in previous works. [34,35] By giving flexibility to the self-assembly process, the rubbery PDMS block facilitates

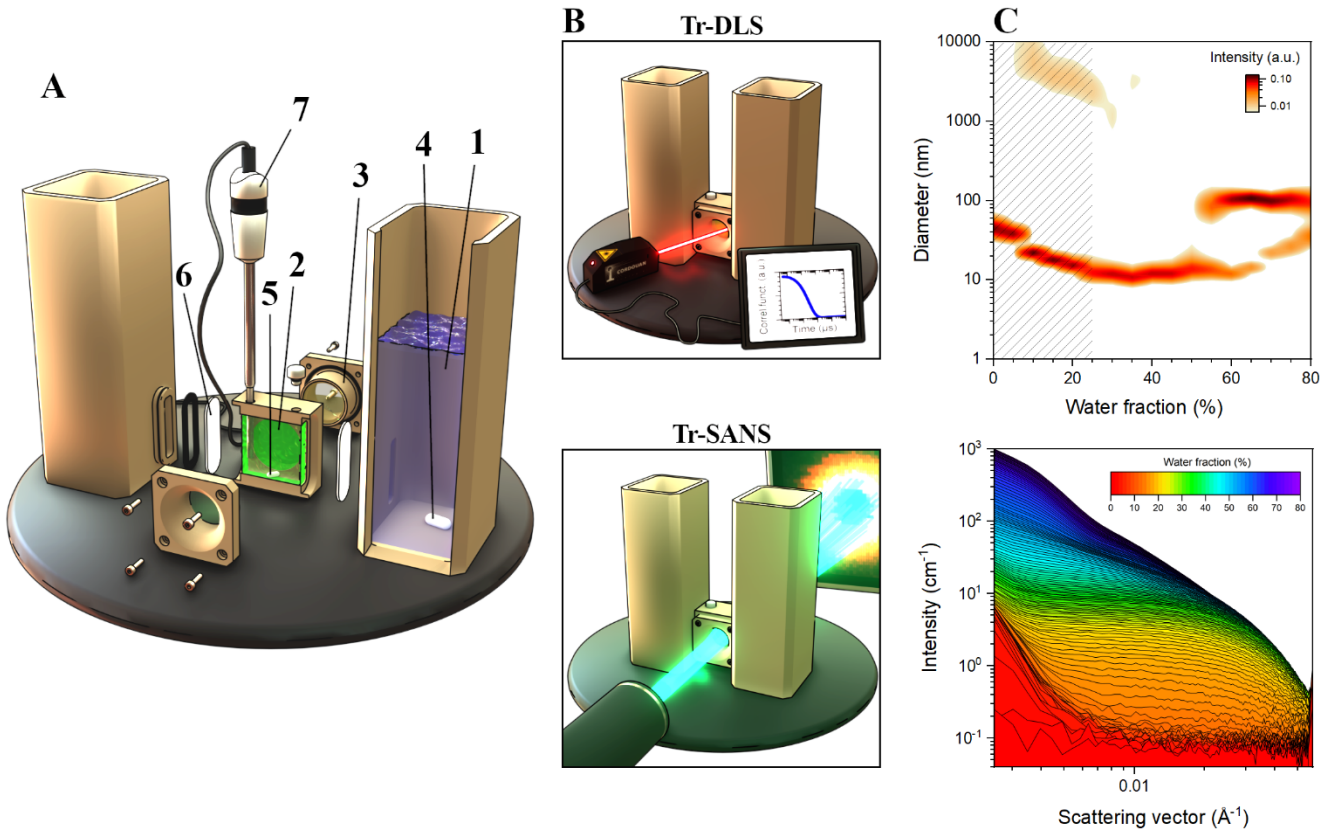

Figure 1. (A) Exploded view of the dialysis setup used for continuous kinetic monitoring of BC self-assembly: ① Lateral reservoirs containing water (2 x 250 mL), ② Measurement cell containing the BC solution in THF (V = 5 mL), ③ Quartz windows (thickness = 2 mm), ④ Reservoir stirring, ⑤ Cell stirring, ⑥ Custom-cut ultrafiltration disc in regenerated cellulose of defined porosity (x 2). ⑦ Conductivity probe. All plastic parts are made in solvent-resistant PEEK. (B) Configuration of the remote DLS (*top*) and SANS (*bottom*) detection. (C) Tr-DLS and Tr-SANS mapping of the dialysis of PDMS27-*b*-PEG17 at 5 g/L in (deuterated) THF against (deuterated) water: hydrodynamic sizes (*top*) and SANS spectra (*bottom*) as function of the water fraction. The scattering contribution due to solvent fluctuations alone was systematically subtracted from the SANS spectra (Figure SX).

vesicle formation under near-equilibrium conditions.

The BC solution in THF was introduced into the scattering cell, which was separated from two water-containing reservoirs by cellulose membranes (Figure 1A). The scattering cell and reservoirs were continuously stirred to allow homogeneous solvent interdiffusion. Importantly, the cell design allowed the BC concentration to be kept constant throughout the dialysis, unlike what is typically achieved with dialysis bags. The addition of 1 mM NaCl in water allowed to monitor the progress of dialysis by conductivity (Figures S1A-S1B). By varying the membrane porosity, the complete solvent exchange can be achieved in less than 10 hours (membrane of 100 kDa) or up to more than 20 hours (membrane of 10 kDa) (Figure S1C). The data presented herein were obtained with PDMS27-*b*-PEG17 (hydrophilic mass fraction, f = 31%) using a 10 kDa membrane for which the water exchange rate is less than 0.1%.min^{-1}, i.e, relatively low to favour BC self-assembly close to thermodynamic equilibrium (Figure S1D).[14,18] Data collected with other copolymer compositions and membrane porosity are provided in the supplementary material and will be discussed later.

A nanoparticle size analyzer combining time-resolved DLS (Tr-DLS) and in situ remote optical probe (VASCO KIN, Cordouan Technologies)[36] was used for kinetic monitoring of the dialysis (Figure 1B and S2). By providing valuable information about the size and size-dispersity of BC aggregates, Tr-DLS gives a first insight into the pathway of vesicle formation. For low water volume fractions (f_w < 25%), DLS measurements were poorly resolved due to almost complete contrast matching of the PDMS blocks in deuterated THF (n_{PDMS} = 1.407, n_{THF} = 1.405). The first detectable structures were 10 nm-diameter aggregates, most likely micellar aggregates, which developed in solution for 25% < f_w < 50%. A second population of 100 nm-diameter aggregates appeared spontaneously at f_w = 55%. Thereafter, micelles grew and tended to fuse with the larger aggregates before the end of dialysis, which was stopped after 22 hours, corresponding to fw = 80%.

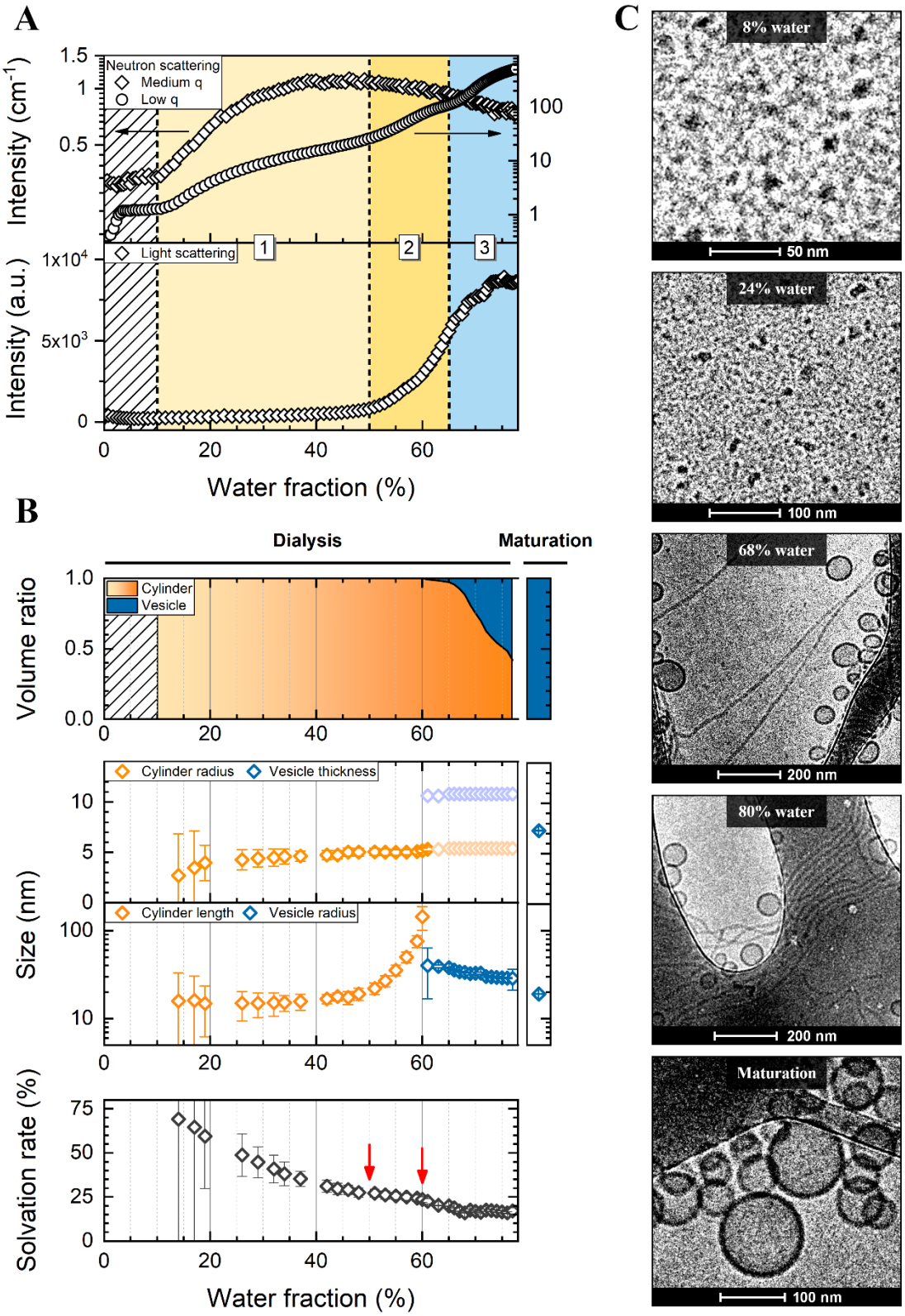

Figure 2. (A) Variation of neutron scattering intensities averaged at low q (0.0025-XXX Å^{-1}) and middle q (XXXX-0.058 Å^{-1}) with water volume fraction. The variation in light scattering intensity (q = 0.0026 Å^{-1}) is also given for comparison. The three main areas of interest are annotated (see text). (B) Main results derived from SANS spectra fitting plotted as function of the water volume fraction: i) volume ratios of the aggregate morphologies, ii) characteristic sizes of BC aggregates, iii) Solvation rate of PDMS blocks in BC assemblies, expressed as the volume fraction of THF-d_8 remaining in the core of aggregates (see supporting information). C) CryoTEM analysis of the dialyzed BC solution at defined water volume fractions.

Solvent exchange was monitored under similar conditions by time-resolved small angle neutron scattering (Tr-SANS) to determine aggregate morphology (Figure 1B). Tr-SANS measurements were performed on the D22 beamline at Institut Laue-Langevin (ILL, Grenoble).

Incident neutrons of 6 Å and a sample-to-detector distance of 17.6 m yielded a range of scattering vectors (q) from 0.0025 $Å^{-1}$ to 0.058 $Å^{-1}$. The time intervals for data collection were set to 15 min with 5 min of accumulation time allowing three samples to be followed at the same time (Picture S1). Typical SANS spectra obtained during dialysis are reproduced in Figure 1C where the color shift highlights the structural changes in BC self-assembly. At the low q-end, the upturn of the scattering intensity for f_w < 10% stems from fluctuations in the solvent composition, which are exacerbated by the presence of the copolymer, as could be verified by running the dialysis without the copolymer (Figure S3). The variation in scattering intensity during dialysis, after subtraction of the solvent contribution, provides a qualitative yet informative insight into BC self-assembly (Figure 2A). For very small water fractions (f_w < 10%) the intensity remained low as also observed by light scattering (LS), consistent with the presence of free copolymer chains or small micelles. Then, the intensity in the mid-q region increased sharply for 10 % < f_w < 40% (region ①), which was attributed to PDMS desolvation leading to BC self-assembly (Figure 2B). The jump in the low-q intensity profile at f_w = 10% confirms that a change in BC morphology has occurred. However, the structures formed in the region ① must be quite small since the LS intensity remained low (Figure 2A). The transition to larger structures actually occurred at 50% < f_w < 65% (region ②), where the low-q and LS intensities increased concomitantly. For f_w > 65% (region ③), the large increase in intensity at low q and the small increase in intensity in LS suggests a change in aggregate shape rather than size.

SANS spectra were fitted with SasView software using a combination of the smallest number of form factors (sphere, cylinder, vesicle) to introduce as few fitting parameters as possible (Figure 2B). Only for f_w < 10% the spectra could not be adequately fitted due to the too low scattered intensity (Figure 2A). However, small spherical micelles (R= 5 nm) could be well detected by cryoTEM at low water contents (f_w = 8%), as shown in Figure 2C. Then, short cylindrical micelles of almost constant size (R = 3-5 nm, L = 15 nm) were fitted in a wide range of water fractions, i.e. between 10% and 50%, where PDMS blocks is gradually desolvated. Cylinders appear to be rather polydisperse, both in size and shape, as seen by cryoTEM (Figure 2c). For f_w > 50% the system enters a critical zone characterized by a steep elongation of cylinders into rod-like micelles, the length of which could be determined by SANS up to 150 nm using this specific configuration (Figure 2B and Figure S5). However, cryoTEM shows that rod micelles reached much greater lengths, in the micron range for f_w > 65%. At the same time, the first vesicles developed in solution, the proportion of which gradually increased with f_w at the expense of the rods. It can be noticed that the vesicle radius decreased slightly from 40 nm at f_w = 65% to 30 nm at f_w = 80%.

When the dialysis was stopped after 22 hours (f_w = 80%), the BC solution contained 60% vesicles and 40% rod-like micelles. The solution was stored for "maturation" during 40 days at room temperature, followed by DLS and then reanalyzed by SANS and CryoTEM. Only vesicles of slightly smaller radius (R = 20 nm) were detected by SANS (Figure S7B) and confirmed by cryoTEM (Figure 2C and S12). The DLS monitoring of the "maturation" process is marked by the slow and progressive fusion of the two populations into a single population attributed to the vesicles (Figure S7A). This suggests that the dynamics of the system is preserved at f_w = 80% to allow vesicle fission contributing to the equilibration of the vesicle size.[18,37]

The overall self-assembly mechanism of PDMS27-*b*-PEG17 upon solvent-to-water exchange is in agreement with previous studies where the spherical micelles → rod-like micelles → vesicles sequence has been reported for various amphiphilic block copolymer systems.[14,19,25] It is consistent with an increase of the interfacial tension of the core-forming PDMS as the solvent polarity increases. Micellar aggregates of spherical shape first form (f_w < 10%) to minimize the total interfacial area, which in turn leads to the core chain stretching as the particles grow. When the entropy penalty associated to the stretching is too high, aggregates must adopt another geometry to relax the stretching, which contributes to decrease the overall free energy of the system.[14,38] As a result, aggregates of reduced curvature (i.e., higher packing density) are successively formed with increasing water content : rod-like micelles for f_w > 10% and vesicles for f_w > 60%. Inverted BC structures previously reported[39,40] cannot form further beyond the vesicular structure due to the reduced mobility of BC chains at high water contents.[14]

The continuous monitoring of solvent exchange using LS/SANS/cryoTEM revealed some important aspects: i) The critical water fraction at which micellization takes places (f_w < 10%) is in the same range as that obtained for PS-*b*-PAA copolymers containing high molar mass PS blocks, thus emphasizing the strong hydrophobic nature of PDMS blocks.[14] No jump in scattering intensity could be associated to the micellization step due to the too low micelle size and isorefractive conditions in the case of LS detection. ii) The variation of SANS intensity at low q allows to identify breaks at f_w = 50% and 65% (Figure 2A) associated to the formation of rod-like micelles and vesicles, respectively. It coincides with small discontinuities found in the variation of the PDMS solvation (red arrows in Figure 2B), thus indicating that morphological transitions are driven by the hydrophobicity changes of the PDMS core. The THF fraction remaining in the vesicle membrane at the end of the dialysis is about 20% which appear to be sufficient to allow vesicle size equilibration, probably through fission pathways. iii) The steep elongation of cylinders into rod-like micelles coincides with the formation of the first vesicles.

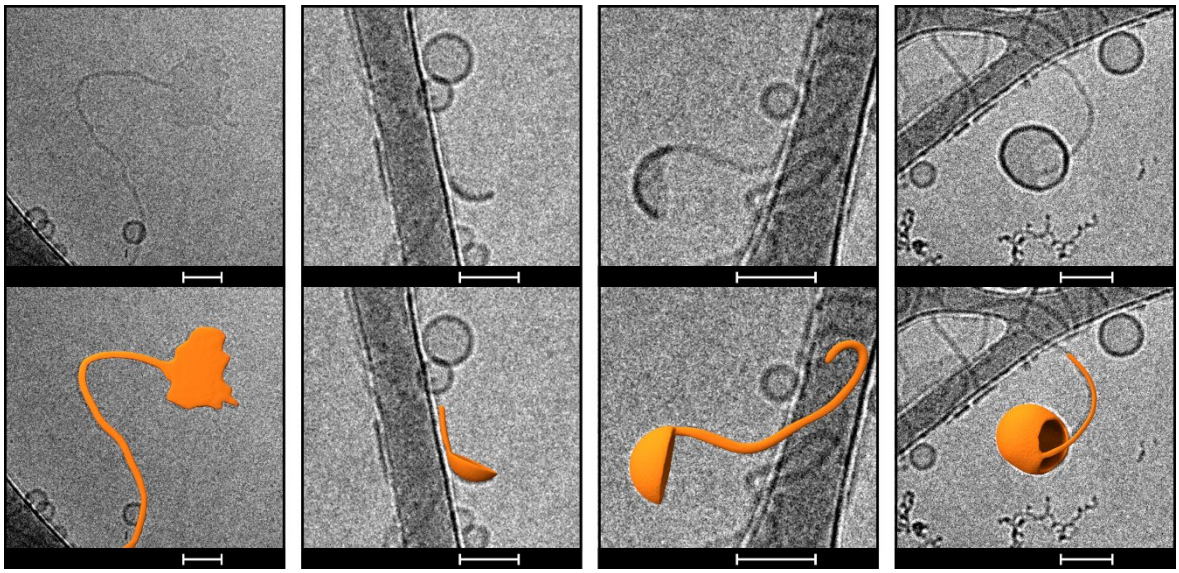

Figure 3. CryoTEM images of the PDMS27-*b*-PEG17 copolymer solution at f_w = 80% illustrating the most probable transition pathway from rod-like micelles to vesicles (scale bar = 100 nm) (*top*). Highlighting of the areas of interest (*bottom*). Three different stages can be distinctly observed from left to right: i) membrane formation at the micelle end-caps, ii) membrane bending, iii) membrane closure.

Clearly, rod-like micelles must be precursors of the vesicles. The possible mechanism by which this change in morphology occurs is shown in Figure 3 where cryoTEM images obtained at f_w = 80% depict the flattening of the rod ends into lamella, followed by the gradual bending of lamella into vesicles, as previously reported theoretically and experimentally.[19,41–44] iv) Equilibration of BC vesicles at f_w = 80% is a slow process, even for low molecular weight BCs containing flexible blocks like PDMS, probably due to the low chain exchange rate at high water content and strong repulsive interaction among BC aggregates.[45] The achievement of a unique vesicular morphology several days after the end of dialysis precludes that, in many situations, BC self-assembly has reached its final steady state.

The shorter PDMS23-*b*-PEG13 copolymer (f = 32%) presents similar morphological changes but the volume fraction of vesicles at the end of dialysis was slightly higher than with the previous BC composition (Figure S17). The vesicle dispersity was also lower, as can be seen from the well-defined oscillations in the mid-q region.

Finally, the influence of the dialysis kinetics on the self-assembly mechanism was studied with PDMS27-*b*-PEG17 using a 100 kDa membrane. In such conditions, 80% of THF was exchanged in less than 8 hours (Figure S1C). The most striking change was the formation of vesicles at f_w = 25% compared to f_w = 65% previously observed with a 10k Da membrane, evidencing that the solvent exchange kinetics strongly impacts the self-assembly pathway (Figure S13). The difference in water exchange rate between the two membranes is especially important at the beginning of the dialysis when the osmotic pressure difference between the cell and the reservoirs was maximal (Figure S1D). The dynamics of the polymer chains is also maximal at the beginning of the dialysis when the THF fraction is high.[18,20,45] Both these conditions probably favor the early BC self-assembly into vesicles following a different pathway among the multiple metastable states that can exist in the free energy landscape of a BC system.[19,46,47] Modifying the membrane porosity is therefore a simple way to perform self-assembly under kinetic or thermodynamic control which can be of interest for many polymer and colloidal systems. In order to form close-to-equilibrium structures, the perturbation rate must be as low as possible at each stage of the self-assembly.

ASSOCIATED CONTENT

Supporting_Information. This material is available free of charge via the Internet at http://pubs.acs.org.

AUTHOR INFORMATION

Corresponding Author

Martin Fauquignon - *Laboratoire de Chimie des Polymères Organiques (LCPO), Université de Bordeaux, CNRS, Bordeaux INP, UMR 5629, F-33600 Pessac, France* ; Email: martin.fauquignon@gmail.com

Christophe Schatz - *Laboratoire de Chimie des Polymères Organiques (LCPO), Université de Bordeaux, CNRS, Bordeaux INP, UMR 5629, F-33600 Pessac, France* ; Email: schatz@enscbp.fr

Authors

Lionel Porcar - *Institut Laue-Langevin (ILL), F-38042 Grenoble, France*

Annie Brûlet - *Laboratoire Léon Brillouin, Commissariat à l'Energie Atomique et aux Energies Alternatives (CEA) Saclay, F-91191 Gif-sur-Yvette, France*

Jean-François Le Meins - *Laboratoire de Chimie des Polymères Organiques (LCPO), Université de Bordeaux, CNRS, Bordeaux INP, UMR 5629, F-33600 Pessac, France*

Olivier Sandre - *Laboratoire de Chimie des Polymères Organiques (LCPO), Université de Bordeaux, CNRS, Bordeaux INP, UMR 5629, F-33600 Pessac, France*

Jean Paul Chapel - *Centre de Recherche Paul Pascal (CRPP), UMR CNRS 5031, Université de Bordeaux, F-33600 Pessac, France*

Marc Schmutz - *Institut Charles Sadron, CNRS, Université de Strasbourg, UPR 2223, F-67034 Strasbourg, France*

Funding Sources

This work was supported by the French National Research Agency (ANR), under the grant ANR--18-CE06-0016 (SISAL project).

REFERENCES

(1) Hamley, I. *Block Copolymers in Solution: Fundamentals and Applications: Hamley/Block Copolymers in Solution: Fundamentals and Applications*; 2005. https://doi.org/10.1002/9780470016985.

(2) Mai, Y.; Eisenberg, A. Self-Assembly of Block Copolymers. *Chem. Soc. Rev.* **2012**, *41* (18), 5969–5985. https://doi.org/10.1039/c2cs35115c.

(3) Karayianni, M.; Pispas, S. Block Copolymer Solution Self-Assembly: Recent Advances, Emerging Trends, and Applications. *J. Polym. Sci.* **2021**, *59* (17), 1874–1898. https://doi.org/10.1002/pol.20210430.

(4) Blanazs, A.; Armes, S. P.; Ryan, A. J. Self-Assembled Block Copolymer Aggregates: From Micelles to Vesicles and Their Biological Applications. *Macromol. Rapid Commun.* **2009**, *30* (4–5), 267–277. https://doi.org/10.1002/marc.200800713.

(5) Tian, M.; Qin, A.; Ramireddy, C.; Webber, S. E.; Munk, P.; Tuzar, Z.; Prochazka, K. Hybridization of Block Copolymer Micelles. *Langmuir* **1993**, *9* (7), 1741–1748. https://doi.org/10.1021/la00031a022.

(6) Choi, S.-H.; Lodge, T. P.; Bates, F. S. Mechanism of Molecular Exchange in Diblock Copolymer Micelles: Hypersensitivity to Core Chain Length. *Phys. Rev. Lett.* **2010**, *104* (4). https://doi.org/10.1103/PhysRevLett.104.047802.

(7) Hayward, R. C.; Pochan, D. J. Tailored Assemblies of Block Copolymers in Solution: It Is All about the Process. *Macromolecules* **2010**, *43* (8), 3577–3584. https://doi.org/10.1021/ma9026806.

(8) Nicolai, T.; Colombani, O.; Chassenieux, C. Dynamic Polymeric Micelles versus Frozen Nanoparticles Formed by Block Copolymers. *Soft Matter* **2010**, *6* (14), 3111–3118. https://doi.org/10.1039/B925666K.

(9) Jain, S.; Bates, F. S. Consequences of Nonergodicity in Aqueous Binary PEO–PB Micellar Dispersions. *Macromolecules* **2004**, *37* (4), 1511–1523. https://doi.org/10.1021/ma035467j.

(10) Discher, D. E.; Eisenberg, A. Polymer Vesicles. *Science* **2002**, *297* (5583), 967–973. https://doi.org/10.1126/science.1074972.

(11) Denkova, A. G.; Mendes, E.; Coppens, M.-O. Non-Equilibrium Dynamics of Block Copolymer Micelles in Solution: Recent Insights and Open Questions. *Soft Matter* **2010**, *6* (11), 2351–2357. https://doi.org/10.1039/C001175B.

(12) Nagarajan, R. "Non-Equilibrium" Block Copolymer Micelles with Glassy Cores: A Predictive Approach Based on Theory of Equilibrium Micelles. *Liq. Films Interfaces Colloidal Dispers.* **2015**, *449*, 416–427. https://doi.org/10.1016/j.jcis.2014.12.077.

(13) Lu, J.; Bates, F. S.; Lodge, T. P. Chain Exchange in Binary Copolymer Micelles at Equilibrium: Confirmation of the Independent Chain Hypothesis. *ACS Macro Lett.* **2013**, *2* (5), 451–455. https://doi.org/10.1021/mz400167x.

(14) Shen, H.; Eisenberg, A. Morphological Phase Diagram for a Ternary System of Block Copolymer PS310-b-PAA52/Dioxane/H2O. *J. Phys. Chem. B* **1999**, *103* (44), 9473–9487. https://doi.org/10.1021/jp991365c.

(15) Battaglia, G.; Ryan, A. J. Effect of Amphiphile Size on the Transformation from a Lyotropic Gel to a Vesicular Dispersion. *Macromolecules* **2006**, *39* (2), 798–805. https://doi.org/10.1021/ma052108a.

(16) Campos-Villalobos, G.; Siperstein, F. R.; Charles, A.; Patti, A. Solvent-Induced Morphological Transitions in Methacrylate-Based Block-Copolymer Aggregates. *J. Colloid Interface Sci.* **2020**, *572*, 133–140. https://doi.org/10.1016/j.jcis.2020.03.067.

(17) Wang, Z.; Yin, Y.; Jiang, R.; Li, B. Morphological Transformations of Diblock Copolymers in Binary Solvents: A Simulation Study. *Front. Phys.* **2017**, *12* (6), 128201. https://doi.org/10.1007/s11467-017-0678-6.

(18) Choucair, A. A.; Kycia, A. H.; Eisenberg, A. Kinetics of Fusion of Polystyrene-b-Poly(Acrylic Acid) Vesicles in Solution. *Langmuir* **2003**, *19* (4), 1001–1008. https://doi.org/10.1021/la026187k.

(19) Han, Y.; Yu, H.; Du, H.; Jiang, W. Effect of Selective Solvent Addition Rate on the Pathways for Spontaneous Vesicle Formation of ABA Amphiphilic Triblock Copolymers. *J. Am. Chem. Soc.* **2010**, *132* (3), 1144–1150. https://doi.org/10.1021/ja909379y.

(20) Bovone, G.; Cousin, L.; Steiner, F.; Tibbitt, M. W. Solvent Controls Nanoparticle Size during Nanoprecipitation by Limiting Block Copolymer Assembly. *Macromolecules* **2022**, *55* (18), 8040–8048. https://doi.org/10.1021/acs.macromol.2c00907.

(21) Bates, F. S.; Fredrickson, G. H. Block Copolymer Thermodynamics: Theory and Experiment. *Annu. Rev. Phys. Chem.* **1990**, *41* (1), 525–557. https://doi.org/10.1146/annurev.pc.41.100190.002521.

(22) Johnson, B. K.; Prud'homme, R. K. Mechanism for Rapid Self-Assembly of Block Copolymer Nanoparticles. *Phys. Rev. Lett.* **2003**, *91* (11), 118302. https://doi.org/10.1103/PhysRevLett.91.118302.
(23) Saad, W. S.; Prud'homme, R. K. Principles of Nanoparticle Formation by Flash Nanoprecipitation. *Nano Today* **2016**, *11* (2), 212–227. https://doi.org/10.1016/j.nantod.2016.04.006.
(24) MacFhionnghaile, P.; Svoboda, V.; McGinty, J.; Nordon, A.; Sefcik, J. Crystallization Diagram for Antisolvent Crystallization of Lactose: Using Design of Experiments To Investigate Continuous Mixing-Induced Supersaturation. *Cryst. Growth Des.* **2017**, *17* (5), 2611–2621. https://doi.org/10.1021/acs.cgd.7b00136.
(25) Fürst, C.; Zhang, P.; Roth, S. V.; Drechsler, M.; Förster, S. Self-Assembly of Block Copolymers via Micellar Intermediate States into Vesicles on Time Scales from Milliseconds to Days. *Self-Assem.* **2016**, *107*, 434–444. https://doi.org/10.1016/j.polymer.2016.09.087.
(26) Knight, J. B.; Vishwanath, A.; Brody, J. P.; Austin, R. H. Hydrodynamic Focusing on a Silicon Chip: Mixing Nanoliters in Microseconds. *Phys. Rev. Lett.* **1998**, *80* (17), 3863–3866. https://doi.org/10.1103/PhysRevLett.80.3863.
(27) Tuzar, Z.; Webber, S. E.; Ramireddy, C.; Munk, P. Association of Polystyrene-Poly(Methacrylic Acid) Block Copolymers in Aqueous Media; 1991; Vol. 32, pp 525–526.
(28) La, S. B.; Okano, T.; Kataoka, K. Preparation and Characterization of the Micelle-Forming Polymeric Drug Indomethacin-Incorporated Poly(Ethylene Oxide)-Poly(β-Benzyl L-Aspartate) Block Copolymer Micelles. *J. Pharm. Sci.* **1996**, *85* (1), 85–90. https://doi.org/10.1021/js950204r.
(29) Vangeyte, P.; Gautier, S.; Jérôme, R. About the Methods of Preparation of Poly(Ethylene Oxide)-b-Poly(ε- Caprolactone) Nanoparticles in Water - Analysis by Dynamic Light Scattering. *Colloids Surf. Physicochem. Eng. Asp.* **2004**, *242* (1–3), 203–211. https://doi.org/10.1016/j.colsurfa.2004.04.070.
(30) Grillo, I. Applications of Stopped-Flow in SAXS and SANS. *Curr. Opin. Colloid Interface Sci.* **2009**, *14*, 402–408. https://doi.org/10.1016/j.cocis.2009.04.005.
(31) Lund, R.; Willner, L.; Richter, D. *Kinetics of Block Copolymer Micelles Studied by Small-Angle Scattering Methods*; Advances in Polymer Science; 2013; Vol. 259, p 158. https://doi.org/10.1007/12_2012_204.
(32) Lund, R.; Willner, L.; Richter, D.; Lindner, P.; Narayanan, T. Kinetic Pathway of the Cylinder-to-Sphere Transition in Block Copolymer Micelles Observed in Situ by Time-Resolved Neutron and Synchrotron Scattering. *ACS Macro Lett.* **2013**, *2* (12), 1082–1087. https://doi.org/10.1021/mz400521p.
(33) Lund, R.; Willner, L.; Pipich, V.; Grillo, I.; Lindner, P.; Colmenero, J.; Richter, D. Equilibrium Chain Exchange Kinetics of Diblock Copolymer Micelles: Effect of Morphology. *Macromolecules* **2011**, *44* (15), 6145–6154. https://doi.org/10.1021/ma200532r.
(34) Dao, T. P. T.; Brûlet, A.; Fernandes, F.; Er-Rafik, M.; Ferji, K.; Schweins, R.; Chapel, J.-P.; Fedorov, A.; Schmutz, M.; Prieto, M.; Sandre, O.; Le Meins, J.-F. Mixing Block Copolymers with Phospholipids at the Nanoscale: From Hybrid Polymer/Lipid Wormlike Micelles to Vesicles Presenting Lipid Nanodomains. *Langmuir* **2017**, *33* (7), 1705–1715. https://doi.org/10.1021/acs.langmuir.6b04478.
(35) Fauquignon, M.; Ibarboure, E.; Le Meins, J.-F. Membrane Reinforcement in Giant Hybrid Polymer Lipid Vesicles Achieved by Controlling the Polymer Architecture. *Soft Matter* **2021**, *17* (1), 83–89. https://doi.org/10.1039/dosm01581d.
(36) Riedl, J. C.; Sarkar, M.; Fiuza, T.; Cousin, F.; Depeyrot, J.; Dubois, E.; Mériguet, G.; Perzynski, R.; Peyre, V. Design of Concentrated Colloidal Dispersions of Iron Oxide Nanoparticles in Ionic Liquids: Structure and Thermal Stability from 25 to 200 °C. *J. Colloid Interface Sci.* **2022**, *607*, 584–594. https://doi.org/10.1016/j.jcis.2021.08.017.
(37) Luo, L.; Eisenberg, A. Thermodynamic Size Control of Block Copolymer Vesicles in Solution. *Langmuir* **2001**, *17* (22), 6804–6811. https://doi.org/10.1021/la0104370.
(38) Zhang, L.; Eisenberg, A. Multiple Morphologies and Characteristics of "Crew-Cut" Micelle-like Aggregates of Polystyrene-b-Poly(Acrylic Acid) Diblock Copolymers in Aqueous Solutions. *J. Am. Chem. Soc.* **1996**, *118* (13), 3168–3181. https://doi.org/10.1021/ja9537095.
(39) Gröschel, A. H.; Walther, A. Block Copolymer Micelles with Inverted Morphologies. *Angew. Chem. Int. Ed.* **2017**, *56* (37), 10992–10994. https://doi.org/10.1002/anie.201703765.
(40) Shen, H.; Eisenberg, A. Block Length Dependence of Morphological Phase Diagrams of the Ternary System of PS-b-PAA/Dioxane/H2O. *Macromolecules* **2000**, *33* (7), 2561–2572. https://doi.org/10.1021/ma991161u.
(41) Chen, L.; Shen, H.; Eisenberg, A. Kinetics and Mechanism of the Rod-to-Vesicle Transition of Block Copolymer Aggregates in Dilute Solution. *J. Phys. Chem. B* **1999**, *103* (44), 9488–9497. https://doi.org/10.1021/jp9913665.
(42) Yamamoto, S.; Maruyama, Y.; Hyodo, S. Dissipative Particle Dynamics Study of Spontaneous Vesicle Formation of Amphiphilic Molecules. *J. Chem. Phys.* **2002**, *116* (13), 5842–5849. https://doi.org/10.1063/1.1456031.
(43) Antonietti, M.; Förster, S. Vesicles and Liposomes: A Self-Assembly Principle Beyond Lipids. *Adv. Mater.* **2003**, *15* (16), 1323–1333. https://doi.org/10.1002/adma.200300010.
(44) Uneyama, T. Density Functional Simulation of Spontaneous Formation of Vesicle in Block Copolymer Solutions. *J. Chem. Phys.* **2007**, *126* (11), 114902. https://doi.org/10.1063/1.2463426.

(45) Zhang, L.; Eisenberg, A. Thermodynamic vs Kinetic Aspects in the Formation and Morphological Transitions of Crew-Cut Aggregates Produced by Self-Assembly of Polystyrene-b-Poly(Acrylic Acid) Block Copolymers in Dilute Solution. *Macromolecules* **1999**, *32* (7), 2239–2249. https://doi.org/10.1021/ma981039f.
(46) Vena, M. P.; de Moor, D.; Ianiro, A.; Tuinier, R.; Patterson, J. P. Kinetic State Diagrams for a Highly Asymmetric Block Copolymer Assembled in Solution. *Soft Matter* **2021**, *17* (4), 1084–1090. https://doi.org/10.1039/D0SM01596B.
(47) Fu, Z.; Wang, Y.; Li, F.; Niu, X.; Li, L.; Liu, D.; Liu, Z.; Guo, X. Access to Different Transient Assemblies through Kinetic Control over the Self-Assembly of Amphiphilic Block Copolymers Using a Versatile Micromixer. *Chem. Eng. Sci.* **2021**, *246*, 116998. https://doi.org/10.1016/j.ces.2021.116998.

SYNOPSIS TOC (Word Style "SN_Synopsis_TOC"). If you are submitting your paper to a journal that requires a synopsis graphic and/or synopsis paragraph, see the Instructions for Authors on the journal's homepage for a description of what needs to be provided and for the size requirements of the artwork.

Authors are required to submit a graphic entry for the Table of Contents (TOC) that, in conjunction with the manuscript title, should give the reader a representative idea of one of the following: A key structure, reaction, equation, concept, or theorem, etc., that is discussed in the manuscript. Consult the journal's Instructions for Authors for TOC graphic specifications.

Insert Table of Contents artwork here